AD-A153 683 NUMERICAL SOLUTIONS OF THE POTENTIAL DISTRIBUTION WITHIN THE VACUUM REGIO..(U) SCIENTIFIC RESEARCH ASSOCIATES INC GLASTONBURY CT F DAVOUDZADEH ET AL. 1/1

UNCLASSIFIED MAR 85 R85-920020-F N00014-83-C-0719 F/G 20/8 NL

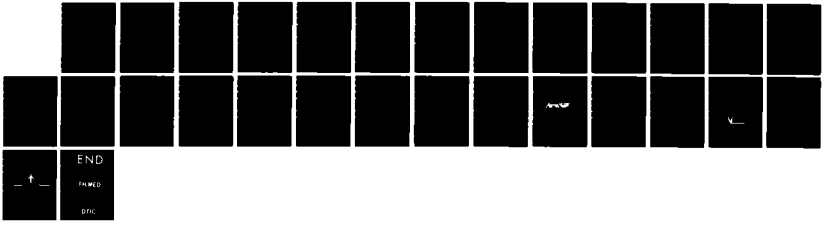

END

FILMED

DTIC

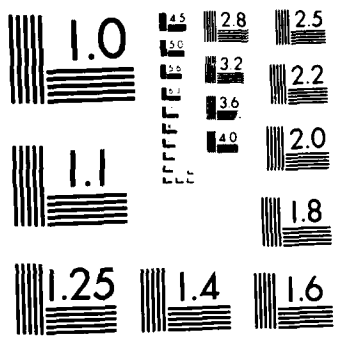

NUMERICAL SOLUTIONS OF THE POTENTIAL DISTRIBUTION WITHIN THE VACUUM REGION OF THE FEATRON

REPORT R85-920020-F

F. DAVOUDZADEH

D.V. ROSCOE

R.C. BUGGELN

H.L. GRUBIN

March 1985

Prepared for the U.S. Naval Research Laboratory

SCIENTIFIC RESEARCH ASSOCIATES, INC.
P.O. BOX 498
GLASTONBURY, CT 06033

REPORT DOCUMENTATION PAGE

1a. REPORT SECURITY CLASSIFICATION Unclassified	1b. RESTRICTIVE MARKINGS
2a. SECURITY CLASSIFICATION AUTHORITY	3. DISTRIBUTION/AVAILABILITY OF REPORT Approved for Public Release Distribution Unlimited
2b. DECLASSIFICATION/DOWNGRADING SCHEDULE	
4. PERFORMING ORGANIZATION REPORT NUMBER(S) R85-920020-F	5. MONITORING ORGANIZATION REPORT NUMBER(S)
6a. NAME OF PERFORMING ORGANIZATION Scientific Research Associates, Inc. 6b. OFFICE SYMBOL (If applicable) 8N189	7a. NAME OF MONITORING ORGANIZATION Naval Research Laboratory
6c. ADDRESS (City, State and ZIP Code) P.O. Box 498 Glastonbury, CT 06033	7b. ADDRESS (City, State and ZIP Code) 4555 Overlook Avenue, S.W. Washington, DC 20375
8a. NAME OF FUNDING/SPONSORING ORGANIZATION Office of Naval Research 8b. OFFICE SYMBOL (If applicable) N00014	9. PROCUREMENT INSTRUMENT IDENTIFICATION NUMBER N00014-83-C-0719
8c. ADDRESS (City, State and ZIP Code) Contracting Officer Code 614A:DHP Dept. of the Navy 800 No. Quincy Street, Arlington, VA 22217	10. SOURCE OF FUNDING NOS. PROGRAM ELEMENT NO. / PROJECT NO. / TASK NO. / WORK UNIT NO.
11. TITLE (Include Security Classification) Numerical Solutions of the Potential Distribution within the Vacuum Region of the "FEATRON"	
12. PERSONAL AUTHOR(S) F.Davoudzadeh, D.V.Roscoe, R.C.Buggeln, H.L.Grubin	
13a. TYPE OF REPORT Final Report 13b. TIME COVERED FROM 83/9 TO 84/10	14. DATE OF REPORT (Yr., Mo., Day) 1985 March 28 15. PAGE COUNT 27
16. SUPPLEMENTARY NOTATION	
17. COSATI CODES FIELD / GROUP / SUB. GR.	18. SUBJECT TERMS (Continue on reverse if necessary and identify by block number) Vacuum, FEATRON, Space Charge, Semiconductor,

19. ABSTRACT (Continue on reverse if necessary and identify by block number)

This report describes the development of a coordinate system generation procedure suitable for use in the numerical prediction of the physical operation of the FEATRON. The suitability of the coordinate system is demonstrated by application to a simplified model of the equations governing charge distribution in the vacuum region of a single FEATRON cell. For this purpose, a solution to Laplace's equation subject to mixed Dirichlet and Neumann boundary conditions is presented. The numerical method used is the Linearized Block Implicit method of Briley and McDonald which is also described.

20 DISTRIBUTION/AVAILABILITY OF ABSTRACT UNCLASSIFIED/UNLIMITED ☒ SAME AS RPT. ☐ DTIC USERS ☐	21. ABSTRACT SECURITY CLASSIFICATION Unclassified
22a NAME OF RESPONSIBLE INDIVIDUAL Dr. Richard F. Greene	22b TELEPHONE NUMBER (Include Area Code) (202) 767-3577 22c OFFICE SYMBOL Code 6830

TABLE OF CONTENTS

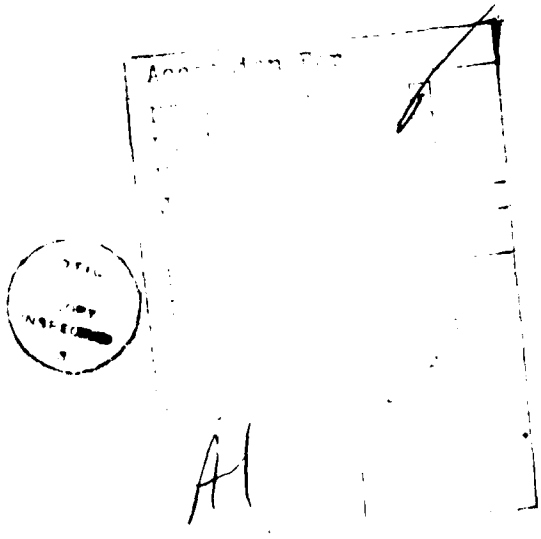

ABSTRACT

This report describes the development of a coordinate system generation procedure suitable for use in the numerical prediction of the physical operation of the FEATRON. The suitability of the coordinate system is demonstrated by application to a simplified model of the equations governing charge distribution in the vacuum region of a single FEATRON cell. For this purpose, a solution to Laplace's equation subject to mixed Dirichlet and Neumann boundary conditions is presented. The numerical method used is the Linearized Block Implicit method of Briley and McDonald which is also described.

I. INTRODUCTION

The purpose of the present study was to develop a coordinate system generation technique for subsequent use in the prediction of the physical operation of the FEATRON shown, schematically, in figure 1. The FEATRON consists of (1) an array of 'cone-shaped' semiconducting emitters, (2) a collector or anode contact, and (3) a metallic grid array that controls the flow of carriers to the collector plate. The grid operates in a manner similar to the grid in a vacuum tube, and the gate in a field effect transistor. Transport within the FEATRON takes place in the vacuum, and the device represents, through its design, a significant coupling of advanced semiconductor technology with the radiation hard features of the vacuum tube. Indeed, the device itself must be regarded as a major advance in vacuum tube technology in which the significant variation in charged particle transport is associated with the geometry of the emitter and the placement of the 'grid-holes'.

The present study is confined to one cell of the FEATRON, shown schematically in figure 2. Within this cell transport is conceptually separated into two distinct parts: (1) carrier transport within the semiconductor, and (2) transport within the vacuum region. Within the semiconductor, Poisson's equation and Maxwell's equations including that of continuity, must be solved along with a set of equations describing carrier transport. Typical length scales for the emitter are of the order of a micron or less and nonequilibrium effects offer the possibility of transient velocity overshoot. Additionally, care is required in treating transport associated with the constraints of the cone tip, particularly with regard to adequately representing the bias dependence of field emission. For the vacuum, transit is governed again by Maxwell's equations, coupled to momentum, energy, and particle balance equations, and relevant scattering interactions. For the vacuum, transit may be simplified through coupling of Poisson's equations to kinetic equations which ignore scattering.

The study performed under Contract N00014-83-C-0719, and summarized below was concerned exclusively with the vacuum region, and represents the first phase of a multifaceted study of the charged particle dynamics of the FEATRON. Specifically, this study was devoted to (1) developing a nonorthogonal coordinate system to smoothly represent the boundaries and interior of one cell of the FEATRON, and (2) demonstrating its effectiveness through solutions to Laplace's equation subject to mixed Dirichlet and Neumann boundary conditions.

A clear, first extention of this study would couple Poisson's equation to charge particle transport within the vacuum section of the one cell FEATRON.

This Report is in seven sections. Section II contains a brief discussion of the coordinate transformation formalism. Section III is a discussion of the algorithm used to solve the problem. A description of the geometry of the boundaries and interior of the vacuum region is summarized in Section IV. Section V displays the solution to Laplaces equation, in the absence of the grid. Section VI introduces the modifications needed to include the grid. The study is summarized in Section VII.

II. COORDINATE TRANSFORMATION

Laplace's equation in Cartesian coordinates is

$$\Delta^2\phi = \frac{\partial^2\phi}{\partial x^2} + \frac{\partial^2\phi}{\partial y^2} + \frac{\partial^2\phi}{\partial z^2} = 0 \tag{1}$$

for the potential ϕ (X,Y,Z). Due to the assumed axisymetric nature of the FEATRON cell simplifications occur through solutions in a two dimensional domain with dependent variables X_1, X_2. The choice of grid for these independent variables is critical for numerical calculations. For example, if the independent variables X_1 and X_2 are established on a Cartesian grid, the grid points for the FEATRON geometry will not necessarily lie on the boundaries. From a numerical standpoint, the potential distribution would require interpolation at the boundaries and could incur spatial truncation errors. These numerical errors are avoided by using a coordinate system that is "fitted" to the geometry of the FEATRON. There is, of course, a tradeoff in introducing curvilinear coordinates. The most significant being that equation (1) is more complicated in form.

The transformation of equation (1) to curvilinear coordinates is direct, and is found in a variety of texts (see, e.g., [1]). For a set of Cartesian variables X_1, X_2, and a set of nonorthogonal curvilinear variables Y_1, Y_2 a set of functional relationships exist whereby,

$$x_1 = x_1(y_1, y_2) \tag{2}$$

$$x_2 = x_2(y_1, y_2) \tag{3}$$

Noting

$$dx_1 = \frac{\partial x_1}{\partial y_1} dy_1 + \frac{\partial x_2}{\partial y_2} dy_2 \tag{4}$$

$$dx_2 = \frac{\partial x_2}{\partial y_2} dy_1 + \frac{\partial x_2}{\partial y_2} dy_2 \tag{5}$$

a requirement on the transformation of equations (1) and (2) is that the Jacobian, equation (6), does not vanish.

$$J = \begin{vmatrix} \frac{\partial x_1}{\partial y_1} & \frac{\partial x_1}{\partial y_2} \\ \frac{\partial x_2}{\partial y_1} & \frac{\partial x_2}{\partial y_2} \end{vmatrix} \neq 0 \tag{6}$$

In terms of the new variables, Laplace's equation is written as

$$\nabla^2\phi = \frac{1}{J}\frac{\partial}{\partial y_1}\left(Jg^{ij}\frac{\partial \phi}{\partial y_i}\right) = 0, \quad \begin{matrix} i = 1,2 \\ j = 1,2 \end{matrix} \tag{7}$$

where

$$g^{ij} = \frac{\partial y_i}{\partial x_k}\frac{\partial y_i}{\partial x_k} \tag{8}$$

and a summation convention is imposed.

Equation (7) with a suitable set of boundary conditions is the equation of interest in this current work. The numerical solutions of equation (7) subject to representative boundary conditions has been achieved using a numerical algorithm which solves the steady state problem represented by equation (7), by solving a transient problem which reduces to the same solution at steady state. This solution procedure is discussed in detail next.

III. SOLUTION PROCEDURE

The solution procedure, summarized below, is based upon the approach of Briley and McDonald [2,3]. Briley and McDonald considered the coupled system of ℓ nonlinear time dependent multidimensional equations, given by

$$\frac{\partial H(\phi_\ell)}{\partial t} = D(\phi_\ell) + S(\phi_\ell) \tag{9}$$

where Φ_ℓ represents a vector of dependent variables. For the present study $\ell=1$, and Φ is the potential in Laplace's equation. S and H are nonlinear functions of Φ_ℓ, and contain no spatial derivatives. $D(\Phi_\ell)$ is a nonlinear multi-dimensional partial differential spatial operator, as given here by the Laplacian. For the problem of interest, S is identically zero and in the steady state, the left side of equation (9) is also zero, yielding a solution to $D(\phi)=0$. To solve equation (9), H is first backward differenced in time. For a fully implicit scheme

$$\frac{H^{n+1} - H^n}{\Delta t} = D^{n+1} + S^{n+1} \tag{10}$$

with $\Delta t = t^{n+1} - t^n$. For a Crank-Nicolson formulation

$$\frac{H^{n+1} - H^n}{\Delta t} = \frac{D^{n+1} + D^n}{2} + \frac{S^{n+1} + S^n}{2} \tag{11}$$

More generally, time differencing about $t^{n+\beta\Delta t}$

$$t^n + \beta(t^{n+1} - t^n) = \beta t^{n+1} + (1-\beta)t^n \tag{12}$$

$$\frac{H^{n+1} - H^n}{\Delta t} = \beta(D^{n+1} + S^{n+1}) + (1-\beta)(D^n + S^n) \tag{13}$$

The operator H,D, and S are then formally linearized about t^n as, e.g.,

$$H(\phi)^{n+1} = H(\phi)^n + \left.\frac{\partial H(\phi)}{\partial \phi}\right|^n \Delta\phi^{n+1} + O(\Delta t^2) \tag{14}$$

$$\frac{\left(\frac{\partial H}{\partial \phi}\right)^{n} \Delta\phi^{n+1}}{\Delta t} = \beta\left[D(\phi)^{n} + S(\phi)^{n} + \left(\frac{\partial D^{n}}{\partial \phi} + \frac{\partial S^{n}}{\partial \phi}\right)\Delta\phi^{n+1}\right] + (1-\beta)(D^{n}+S^{n}) \quad (15)$$

$$\left(\frac{\partial H^{n}}{\partial \phi} - \beta\frac{\partial D^{n}}{\partial \phi}\Delta t\right)\Delta\phi^{n+1} = \left(D^{n}+S^{n}\right)\Delta t + \beta\left(\frac{\partial S^{n}}{\partial \phi}\right)\Delta\phi^{n+1}\,\Delta t \quad (16)$$

or

$$\left[\left(\frac{\partial H^{n}}{\partial \phi} - \beta\Delta t\,\frac{\partial S}{\partial \phi}\right) - \beta\frac{\partial D^{n}}{\partial \phi}\Delta t\right]\Delta\phi^{n+1} = \left(D^{n}+S^{n}\right)\Delta t \quad (17)$$

Thus at each grid point, the nonlinear system of coupled PDE's is reduced to a block of $\ell x \ell$ coupled linear system of temporal difference equations, which upon spatial differencing are solved once each time step. Note, for the solution to Laplace's equation $\ell=1$. Additionally, since the linearization error is at worst of the same order as the temporal discretization error, the linearization is not expected to introduce significant inaccuracies.

Application of equation (16) to second order PDE's in one space dimension using standard three-point spatial difference approximations requires the solution of one block $\ell x \ell$ tridiagonal system per time step. Such a system can be solved efficiently using standard block-tridiagonal elimination procedures. However, application of the LBI algorithm given by equation (16) through (18) to multidimensional problems results in the loss of the narrow, block banded matrix structure obtained in one space dimension. The discretization of the multidimensional spatial operator results in a broad-banded structure, which, if solved by direct or iterative methods, can be extremely inefficient. Such observations led Briley and McDonald [2, 3] to develop consistently split LBI algorithms for mutidimensional problems. The splitting is accomplished by dividing the multidimensional spatial operator, L,

$$L \equiv -\beta\frac{\partial D}{\partial \phi}\bigg|^{n} \quad (18)$$

into one dimensional operators associated with each coordinate direction.

$$L = L_x + L_y + L_z \tag{19}$$

Equation (5) is then split following the scalar ADI development of Douglas and Gunn [4]:

$$(A + \Delta t L_x)\Delta\phi^* = \Delta t\left[D(\phi^n) + S(\phi^n)\right] \tag{20a}$$

$$(A + \Delta t L_y)\Delta\phi^{**} = A\Delta\phi^* \tag{20b}$$

$$(A + \Delta t L_z)\Delta\phi^{***} = A\Delta\phi^{**} \tag{20c}$$

In the above

$$A \equiv \left(\frac{\partial H}{\partial \phi}\right)^n - \beta\Delta t\left(\frac{\partial S}{\partial \phi}\right)^n \tag{21}$$

and, $\Delta\phi^*$, $\Delta\phi^{**}$ and $\Delta\phi^{***}$ are intermediate solutions of equations (20a) through (20c).

Again, if three point operators are used to approximate the spatial operators, L_i, each of equations (20a) through (20c) will be block $\ell\times\ell$ tridiagonal, and can be efficiently solved. The block size and band width are independent of the number of grid points, hence the computational effort required to solve the sequence varies linearly with the total number of grid points regardless of the number of space dimensions considered. Elimination of the intermediate steps in equations (20a) through (20c) yields

$$(A+\Delta t L_x)A^{-1}(A+\Delta t L_y)A^{-1}(A+\Delta t L_z)\Delta\phi^{***} = \Delta t\left[D(\phi^n) + S(\phi^n)\right] + O(\Delta t^2) \tag{22}$$

thus

$$\Delta\phi^{n+1} = \Delta\phi^{***} + O(\Delta t^3) \tag{23}$$

However, for two dimensional problems, equation (20c) is omitted, thus

$$\Delta\phi^{n+1} = \Delta\phi^{**} + O(\Delta t^3) \tag{24}$$

The development given above presents a brief outline of the LBI method used in the present investigation. A more detailed development, as well as in-depth discussion of LBI methods, the linearization procedure, and related topics may be found in the article by Briley and McDonald [2].

It should be noted that in applying the above procedure to the solution of Laplace's equation (ℓ=1) a scalar system results and the single element of the A matrix as defined by equation (21) is zero. Thus, the procedure outlined above cannot be directly applied to solve Laplace's equation. However, this problem can be circumvented by adding a pseudo time term to Laplace's equation and marching in this pseudo time space to a steady state. The steady state solution thus generated satisfies Laplace's equation and is the desired solution. Additionally, the pseudo time step can be varied in a manner which accelerates convergence to the steady state resulting in an efficient solution technique.

For the more general problem of transport within the FEATRON, the application of the LBI procedure outlined above to the relevant, time dependent transport equations coupled to Poisson's equation is also not a straight forward task. The direct application of LBI procedures to this system yields an A matrix of the form

$$A = \left|\begin{array}{cc|c} x & x & x \\ x & x & x \\ \hline 0 & 0 & 0 \end{array}\right| \tag{25}$$

which is singular, due to the absence of a time derivative in Poisson's equation. While this does not create problems if only one dimensional solutions are to be computed, for multidimensional solutions this singularity makes it impossible to apply the ADI splitting given by equation (20) to this system, and an alternative must be sought. One alternative is to again introduce artificial time derivatives in each equation. For example, in Poisson's equation, the artifical time derivative yields

$$\frac{\partial\phi}{\partial t} + \nabla^2\phi = S \tag{26}$$

The physical time derivatives in the other governing equations are then treated as source terms, and the artificial time derivatives track the development of the solution variables in an iteration space. Such "iterative" LBI schemes can be highly efficient for generating steady solutions to coupled systems of

nonlinear PDE's since the artificial time step can be chosen to maximize the convergence rate. It is noted, however, that for transient applications such an approach would require that a computational effort of the order of that required to generate a steady state solution be expended at each physical time step. This would obviously result in highly excessive computation time, and would be impractical. Another approach [5], which has been used successfully, is to reformulate the system of governing equations in such a manner that Poisson's equation can be decoupled as is suggested by the partitioning of the A matrix shown in equation (25). This allows the time dependent governing equations to be solved efficiently, without iteration, using an LBI scheme, followed by solution of Poisson's using the approach discussed previously for Laplace's equation. Such an approach can be used to examine transport with the FEATRON, where additional work should concentrate on implementing the moments of the Boltzmann transport equation for studying carrier transport within the structure.

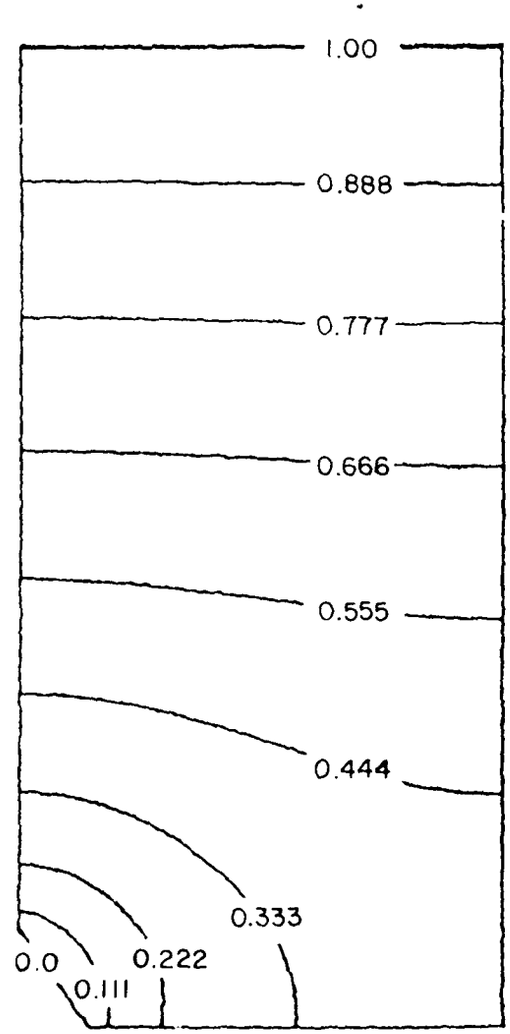

FIGURE 5. FINAL POTENTIAL DISTRIBUTION

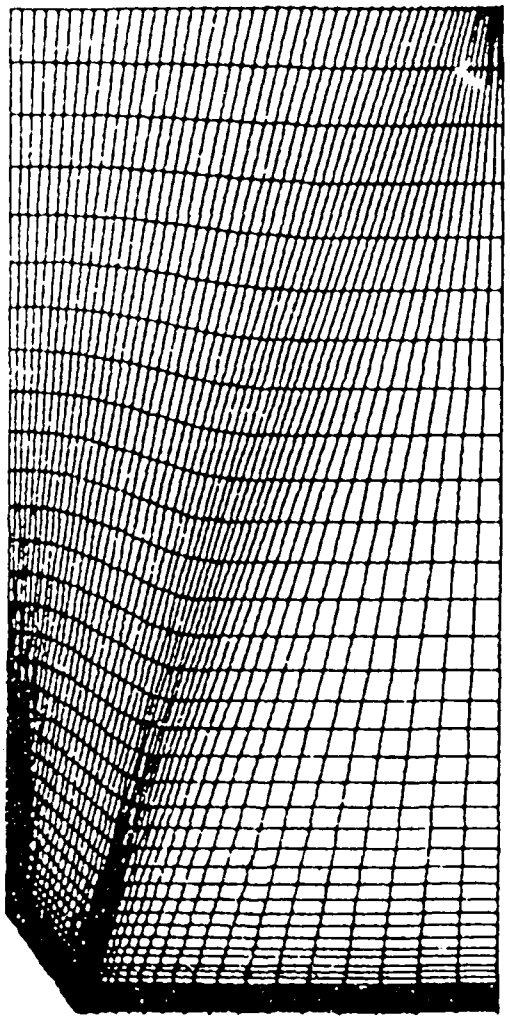

FIGURE 4. GRID DISTRIBUTION FOR A FEATRON CELL

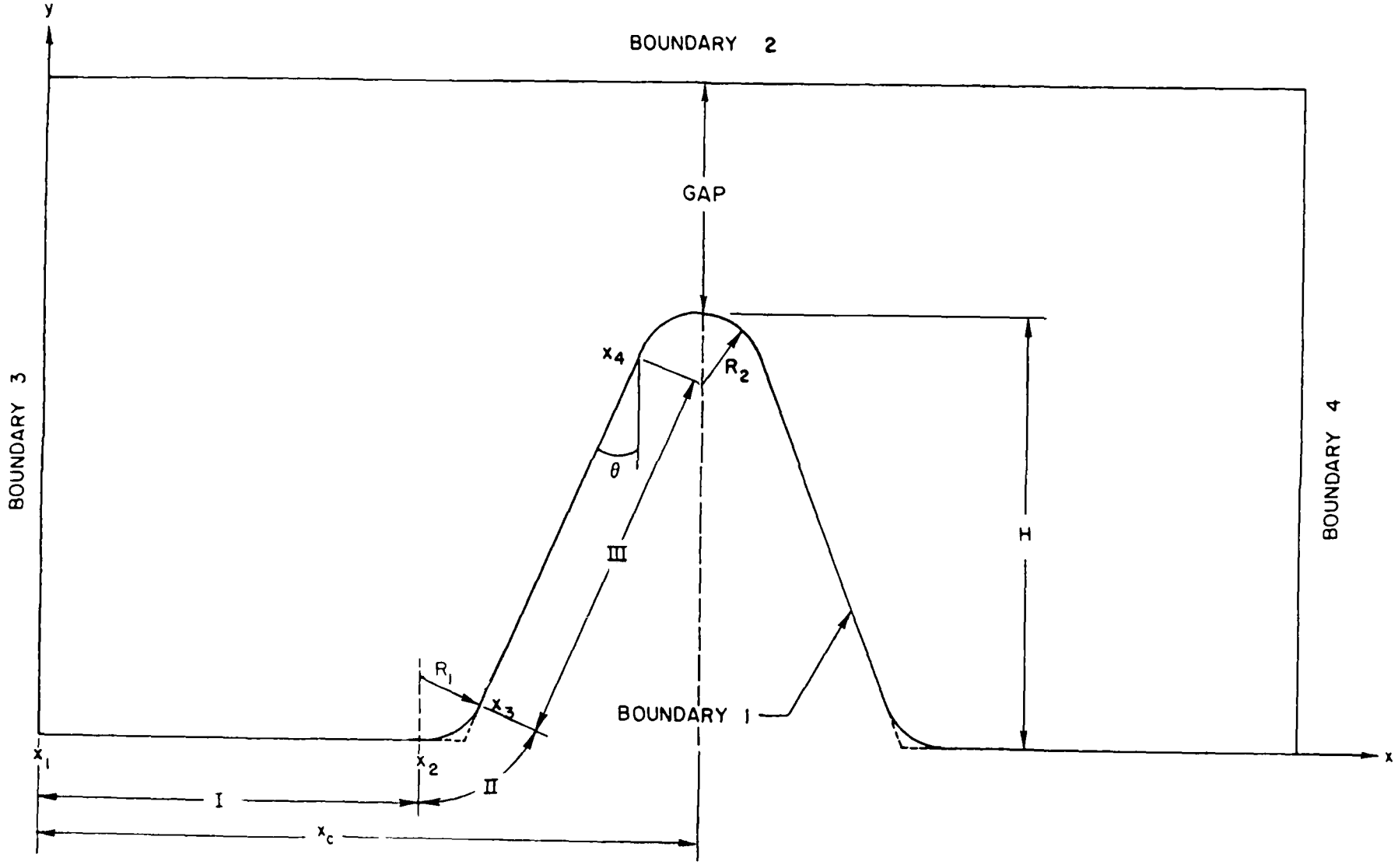

FIGURE 3. SCHEMATIC OF THE **FEATRON** DEVICE SHOWING THE RELEVANT DIMENSIONS OF THE PROBLEM

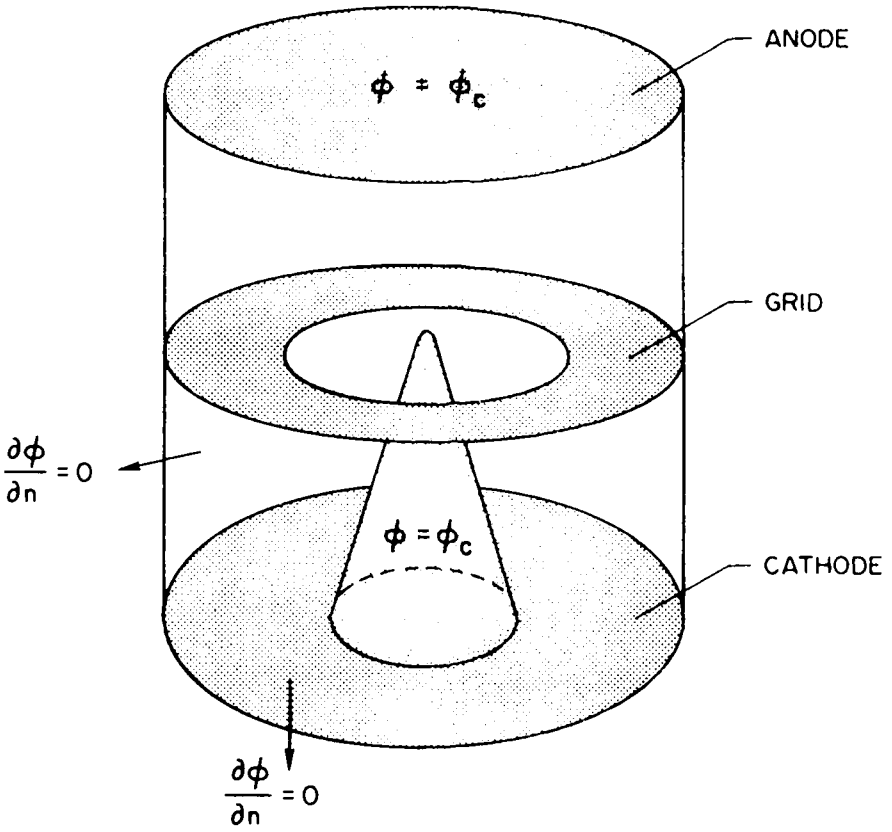

FIGURE 2. SCHEMATIC OF ONE CELL OF THE FEATRON TUBE

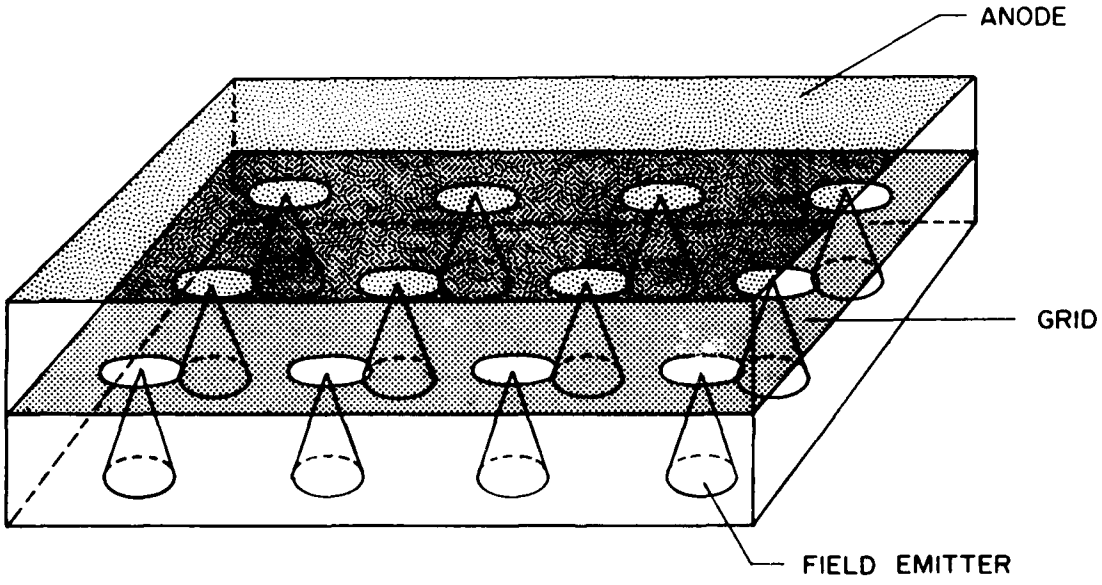

FIGURE I. SCHEMATIC OF THE FEATRON TUBE

DISTRIBUTION LIST

Scientific Officer Naval Research Laboratory Attn: R.F. Greene Code 6830 4555 Overlook Avenue, S.W. Washington, DC 20375	1
Administrative Contracting Officer Defense Contract Administration Services Management Area - Hartford Code S0701A 96 Murphy Road Hartford, CT 06114	1
Director, Naval Research Laboratory Attn: Code 2627 4555 Overlook Avenue Washington, DC 20375	6
Defense Technical Information Center Building 5, Cameron Station Alexandria, VA 22314	12

REFERENCES

1. Sokolnikoff, I.S., Tensor Analysis: Theory and Applications to Geometry and Mechanics of Continua, 2nd Edition, John Wiley, New York, 1964.

2. Briley, W.R., and McDonald, H.: Solution of the Multidimensional Compressible Navier-Stokes Equations by a Generalized Implicit Method. J. Comp. Physics, Vol. 24, No. 4, August 1977, p 373.

3. Briley, W.R., and McDonald, H.: On the Structure and use of Linearized Block Implicit Schemes. J. Comp. Physics, Vol. 34, 1980, p 54.

4. Douglas, J., and Gunn, J.E.: A General Formulation of Alternating Direction Methods. Numerische Math., Vol. 6, 1964, p 428.

5. Scientfic Research Associates, Inc. (SRA) Report 940003-F, August 1984.

6. Scientfic Research Associates, Inc. (SRA) Report 920016-F, January 1985.

7. Oh, Y.N.: An Analytic Transformation Technique for Generating Uniformly Spaced Computational Mesh. Final Report, NASA Lnagley Research Grant NSG 1087, October 1978.

VII. SUMMARY AND PROPOSED FUTURE DIRECTIONS

The objective of the present study was to design and implement a coordinate system and grid structure to represent the constrained design of one cell of the semiconductor/vacuum FEATRON device. The task was undertaken to enable a numerical study of the space and time dependent operational properties of the FEATRON. The objectives of the study were successful.

To undertake future studies of the transient characteristics of the FEATRON, it is necessary to establish a set of relevant governing transport equations. In this case, there are two regions of study, the semiconductor tip and the vacuum region. It is suggested that the next step in the FEATRON simulation involve solutions of the transport equations within the vacuum region. Here two approaches may be taken. The simplest is to assume a kinetic equation within the vacuum that ignores scattering, and to solve this equation simultaneously with Maxwell's electromagnetic equation. This approach has been discussed in the past and is part of most undergraduate texts. A more careful approach involves obtaining solutions to the Boltzmann transport equation simultaneously with Maxwell's equations. Workers at SRA have had a broad range of experience in obtaining approximate solutions to the Boltzmann transport equation through its moments. These equations include the continuity, momentum, and energy balance equations and incorporate the influence of collisons [6]. These moments equations are for multispecie transport, which in the present case, would incorporate the transport of emitted electrons and any other charged particles specific to the vacuum region. It is suggested that these equations be used to study transport within the FEATRON.

The goals of such a study would include examining the time dependent large signal behavior of the FEATRON with such output as power and efficiency. The dependency of the power and efficiency of the FEATRON on design parameters, for an assumed set of boundary conditions representative of carrier emission from the FEATRON tip, would also be studied. The coordinate system to be used for this study has already been developed and would minimize numerical errors associated with the highly constrained FEATRON tip.

SECTION VI. ALGORITHM MODIFICATION FOR INCLUSION OF THE METALIC GRID

The only detailed calculation performed involved the solution to Laplace's equation. However, in anticipation of future studies, modification of the grid generation strategy was introduced to incorporate the grid. Figure 6 shows an example of a coordinate system in which a FEATRON grid has been included. This coordinate system is designed to concentrate points in regions of anticipated high potential gradient. The code used to generate this mesh has been written to facilitate examination of alternative designs by allowing for changes of the grid distribution through modification of the code input parameters.

SECTION V. SOLUTIONS TO LAPLACE'S EQUATION

Laplace's equation governing the potential $\phi(x,y)$ in the field a single cell of the FEATRON device has been solved subject to the following boundary conditions: (see also figure 2)

(i) Fixed potential on the collector ($\phi=\phi c$)

(ii) Fixed potential on the emitter ($\phi=\phi e$)

(iii) On all the surfaces, the first derivative of potential in the direction normal to the surface is set to zero.

It should be noted that in this initial phase of the work, the metallic control grid shown in figure 2 has been omitted from the calculations. Also, even though the emitter tip is a semiconductor and as such would not sustain a fixed potential, in the absence of a suitable model for the tip potential distribution, a fixed potential was assumed. No additional numerical difficulties are incurred by including appropriate boundary conditions, obtained from a model for the tip region physics.

Figure 4 shows the computational coordinate system used in the current calculation. Figure 5 shows the potential distribution obtained by performing the calculation described in this report. In view of the axisymmetric nature of the problem only half of a FEATRON cell has been shown. In the immediate vicinity of the emitter a relatively large potential gradient exists. The field is two dimensional in nature decaying to a linearly varying almost on dimensional distribution in the vicinity of the collector. This result is qualitatively as anticipated and serves to illustrate the validity of the approach developed under this effort.

The technique used in this study is to constrain the values of the physical coordinate, y_{c_k}, at specific values of the computational coordinate, η_{c_k}. At interior points, the η_{c_k}'s are referred to as interior cluster points. In this formulation, two pivot points are associated with each interior cluster point and one pivot point is associated with each end cluster point (η_{pmin} and η_{pmax}). Thus, if there are k interior cluster points, the total number of pivot points is N=2k+2. To determine the functional relationship $y(\eta)$ described in equation (40), requires (if the values of η_{p_j} and αj are prescribed) that the values of the N+1β's in that equation be calculated. Both equation (40) and equation (39) are linear equations with respect to the β's. By constraining the values of the physical coordinates at the interior and end cluster points, k+1 linear independent equations in the β's are obtained. By further constraining the values of hte slope, $f(\eta)$, at the interior and end cluster points, a further k+2 linear indpendent equations for the N+1=2k+3β's. This system is solved for the β's by standard Gaussian elimination techniques and, hence, all the constants of equation (3) are uniquely determined.

There are several advantages to the use of the series of complimentary error functions:

(1) $f(\eta)$ is positive finite and non-zero, i.e., y will always increase with increasing η.

(2) $f(\eta)$ is continuous and successively differential and integrable; and

(3) If the pivot points are spaced at a greater distance, (in computational space) than $\alpha/2$ from each other, the complimentary error functions will have minimal interaction. Thus, the width and location of a complimentary error function can be changed without effecting other complimentary error functions.

(c) Internal Grid Distribution

After boundary grid points are distributed, the coordinates within the interior of the computational domain are constructed. This is achieved by connecting corresponding points on the top and bottom surfaces by straight lines. In general, these lines are not perpendicular to the top and bottom surfaces, but rather inclined to minimize the nonorthogonality at the emitter surface, as seen in figure 4.

The second family of coordinate curves is then determined by distributing along each of the lines of the first family according to a normalized distribution designed to concentrate points near the emitter boundary where large potential gradients are expected.

which can be integrated to yield

$$y = \int_{\eta_{min}}^{\eta} f(\eta)d\eta + y_{min} \tag{38}$$

$S(\eta)$ is chosen to be a series of N complimentary error functions of the form

$$f(\eta) = \frac{dy}{d\eta} = \beta_0 + \frac{1}{2}\sum_{j=1}^{N}\left\{\text{erfc}\left[\frac{\gamma}{\alpha_j}(\eta - \eta_{P_j})\right] - \left[1 + \text{sign}(\alpha_j)\right]\right\}\beta_j \tag{39}$$

The j^{th} complimentary error function is centered in computational space at location η_{P_j} (which is referred to as a pivot point), and α_j is the width in computational space in which 90% of the grid size variation takes place. At computational space location η_{P_j}, the value of $f(\eta)$ assumes a local maximum. γ is a scaling constant for α_j(γ=1.63x2=2.326), erfc (1.163)=0.10) and in the limit as $\alpha_j \to 0$, β_j is the j^{th} step height for pivot j, i.e., the difference in grid spacing on either side of η_{P_j}.

Substitution of equation (39) into equation (38), and integrating yields

$$y - y_{min} = \beta_0(\eta - \eta_{min}) + \sum_{j=1}^{N}\frac{1}{2}\left\{\frac{\alpha_j}{\gamma}\left[\theta_j(\eta) - \theta(\eta_{min})\right] - \left[1 + \text{sign}(\alpha_j)\right]\left[\eta - \eta_{min}\right]\right\}\beta_j \tag{40}$$

where

$$\theta_j(\eta) = \frac{\gamma}{\alpha_j}(\eta - \eta_{P_j})\,\text{erfc}\left[\frac{\gamma}{\alpha_j}(\eta - \eta_{P_j})\right] - \frac{1}{\sqrt{\pi}}\,e^{-\left[\gamma/\alpha_j(\eta - \eta_{P_j})\right]^2} \tag{41}$$

Section III $(x_3 \le x_i \le x_4;\ y_3 \le y_i \le y_4)$

$$x_i = x_3 + (S_i - S_3)\sin\theta \tag{32}$$

$$y_i = y_3 + (S_i - S_3)\cos\theta \tag{33}$$

$$y_4 = H - R_2(1 - \sin\theta) \qquad [99.79 \times 10^{-6}\,\text{cm}]$$

$$x_4 = x_3 + (y_4 - y_3)\tan\theta \qquad [0.4996\ \ 10^{-6}\,\text{cm}]$$

$$s_4 = s_3 + (y_4 - y_3)/\cos\theta$$

Section IV $(x_4 \le x_i \le x_5;\ y_4 \le y_i \le y_5)$

$$x_i = x_4 + R_2\left[\cos\theta - \cos(\theta + \phi_1)\right] \tag{34}$$

$$y_i = y_4 + R_2\left[\sin(\theta + \phi_1) - \sin\theta\right] \tag{35}$$

$$\theta_1 = (S_1 - S_4)/R_2 \tag{36}$$

$$x_5 = x_4 + 2R_2\cos\theta \qquad [0.5 \times 10^{-3}\,\text{cm}]$$

$$y_5 = y_4 \qquad [99.79 \times 10^{-6}\,\text{cm}]$$

$$s_5 = s_4 + R_2(\pi - 2\theta)$$

(b) Distribution of Grid Points on the Boundaries

After the surfaces are analytically defined, grid points are positioned on the boundaries. The number of grid points is chosen to be sufficient to yield required resolution of the potential and of the boundary geometry. This requires, for example, clusters of grid points on Sections 2 and 6.

Transformation Function

The distribution of grid points on boundaries is accomplished by use of a transformation technique described in [7]. If y and η designate the independent variables in physical and computational (grid point) space, respectively, a transformation function is introduced:

$$f = \frac{dy}{d\eta} \tag{37}$$

IV. DESCRIPTION OF THE BOUNDARIES

To achieve numerically accurate and economical solutions it is necessary to (1) describe the boundaries accurately, (2) distribute grid points smoothly along the boundaries, and (3) construct the grid inside the computational domains. The boundary description follows.

(a) Boundary Description

With reference to figure 3, there are four boundaries to consider. The most complex is Boundary 1, and is described in detail below.

Boundary 1:

Section I $(x_1 \le x_i \le x_2)$

$$y_i = 0 \tag{27}$$

$$x_i = x_1 + S_i \tag{28}$$

where S_i is the accumulated arc length along Boundary I.

$x_1 = 0$

Section II $(x_2 \le x_i \le x_3 ; \quad y_2 \le y_i \le y_3)$

$$y_i = y_2 + R_1(1 - \cos \phi_i) \tag{29}$$

$$x_i = x_2 + R_1 \sin \phi_i \tag{30}$$

$$\phi_i = (S_i - S_2)/R_1 \tag{31}$$

where ϕ_i is the angle subtended at the center of the circular arc fillet by radial lines through point (x_2, y_2) and the current location (x_i, y_i).

$x_2 = x_3 - R_1 \cos \theta$ $\left[42.2058 \times 10^{-3} \text{cm}\right]$

$y_2 = 0$

$x_3 = x_c - H - \left[R_2(1 - \sin\theta) - y_3\right] \tan\theta$ $\left[43.0145 \times 10^{-3} \text{cm}\right]$

R_1 is the radius of fillet (see figure 3) $\left[0.1 \times 10^{-6} \text{ cm}\right]$

R_2 is the radius of the tip $\left[0.5 \times 10^{-6} \text{ cm}\right]$

θ is half the cone angle $\left[36°\right]$

H is the cone height $\left[10^{-4} \text{ cm}\right]$

$y_3 = y_2 + R_1(1 - \sin\theta)$ $\left[4.1221 \times 10^{-6} \text{ cm}\right]$

x_c is the x coordinate of the cone center line $\left[0.5 \times 10^{-3} \text{ cm}\right]$

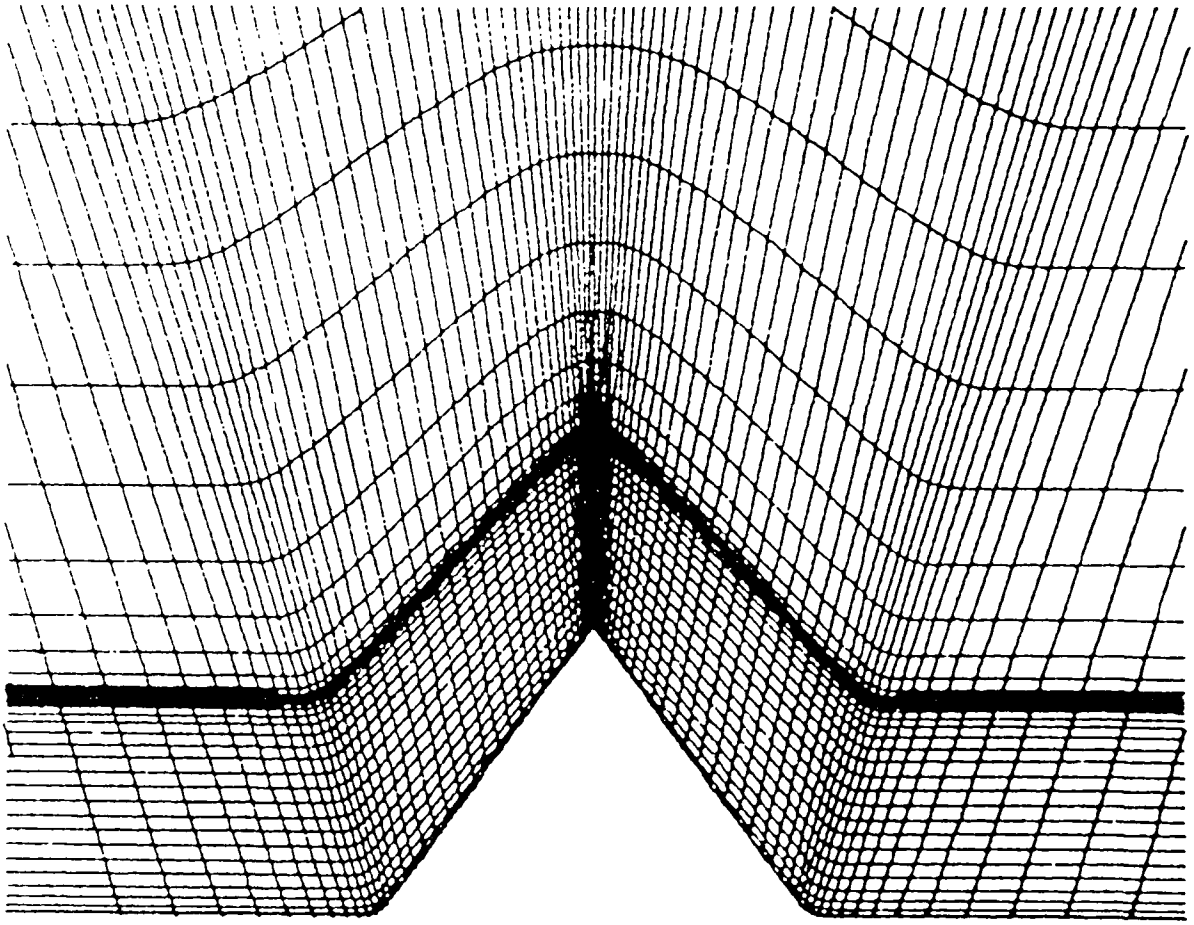

FIGURE 6. SUGGESTED GRID DISTRIBUTION FOR THE FEATRON WITH GRID PLANE

END

FILMED

6-85

DTIC